Korean Chem. Eng. Res., 62(3), 253-261 (2024)
https://doi.org/10.9713/kcer.2024.62.3.253
PISSN 0304-128X, EISSN 2233-9558

Investigation of Temperature Effect on Electrode Reactions of Molten Carbonate Electrolysis Cells and Fuel Cells using Reactant Gas Addition Method

Samuel Koomson and Choong-Gon Lee†

Department of Chemical & Biological Engineering, Hanbat National University,
125 Dongseodaero, Yuseong-gu, Daejeon, 34158, Korea
(Received 9 May 2024; Received in revised from 26 June 2024; Accepted 26 June 2024)

Abstract – The impact of temperature on electrode reactions in 100 cm^2 molten carbonate cells operating as Fuel Cells (FC) and Electrolysis Cells (EC) was examined using the Reactant Gas Addition (RA) method across a temperature range of 823 to 973 K. The RA findings revealed that introduction of H_2 and CO_2, reduced the overpotential at Hydrogen Electrode (HE) in both the modes. However, no explicit temperature dependencies were observed. Conversely, adding O_2 and CO_2 to the Oxygen Electrode (OE) displayed considerable temperature dependencies in FC mode which can be attributed to increased gas solubility due to the electrolyte melting at higher temperatures. In EC mode, there was no observed temperature dependence for overpotential. Furthermore, the addition of O_2 led to a decrease in overpotential, while CO_2 addition resulted in an increased overpotential, primarily due to changes in the concentration of O_2 species.

Key words: Molten carbonate, Fuel cell, Electrolysis cell, Reactant gas addition, Mass transfer, Temperature

1. Introduction

Molten Carbonate Cells (MCCs) have emerged as promising technologies in high-temperature electrochemical energy conversion from H_2 to power in fuel cell mode and vice versa in electrolysis mode. Their distinct attributes, such as their capacity to function at lower temperatures compared to solid oxide cells and their ability to utilise a broad array of fuels, render them appealing choices for efficient power generation and converting excess electricity into chemical fuels. This research group has recently published several works [1-3] that contributed to understand various aspects of MCC systems. This paper explores the critical role of temperature in shaping the electrode reactions within Molten Carbonate Fuel Cells (MCFCs) and Electrolysis Cells (MCECs) by employing the Reactant Gas Addition (RA) method.

Several works on the effect of temperature on MCFCs have been done over the past few years. For example, Saito *et al.* studied the influence of temperature on the performance of 25 cm^2 planar MCFCs and suggested an optimum operating temperature of 948 K [4]. The temperature dependence on performance of MCFCs operated using Li-Na and Li-K electrolytes were compared by Morita *et al.,* who reported a significant overall overpotential in Li-Na cells compared to Li-K cells at temperature ≤ 873 K due to lower oxygen solubility in the Li-Na electrolyte [5]. A numerical study by Musa *et al.* reported that the operating temperature has a significant effect on internally reformed (IR) MCFCs compared to externally reformed (ER) MCFCs owing to the increased production of H_2 gas *via* the reforming reaction at higher temperature [6]. Also, investigations of the dependence of the Hydrogen Electrode (HE) [7] and Oxygen Electrode (OE) [8] reactions on temperature were studied by this group using 100 cm^2 MCFCs operated between the temperature range of 823 to 973 K. The authors reported that the gas-phase mass transfer of the hydrogen electrode resistance was significantly affected by temperature, while no clear dependence was observed at the OE. They further stated that the liquid-phase mass transfer resistance at the OE was immensely influenced by temperature.

On the other hand, very few works on temperature dependency of MCECs are reported. Hu *et al.* explicitly studied the performance [9,10] and electrode reaction characteristics [11,12] of 3 cm^2 MCECs at a temperature range of 873 to 948 K. The authors stated that the overpotential was reduced more in EC mode than in FC mode at all temperatures. Similar observations were reported by Perez *et al.* when 80 cm^2 MCCs were operated reversibly at a temperature range of 843 to 923 K [13]. Audasso *et al.* reported a significant dependence of temperature on the charge transfer resistance and less on mass transfer resistance when 100 cm^2 MCCs were operated reversibly between a temperature range of 893 to 943 K [14]. Also, this group also studied the temperature dependence on the gas-phase and liquid-phase mass transfer resistances at the MCC electrodes operated reversibly using an Inert Gas Step Addition (ISA) method [3].

Temperature plays a pivotal role in shaping the electrode reactions within MCFCs and MCECs. The influence of temperature can be categorised into three key aspects: thermodynamics, reaction kinetics, and mass transfer. Understanding how temperature affects these critical aspects is crucial for optimising the performance and efficiency

† To whom correspondence should be addressed.
E-mail: leecg@hanbat.ac.kr

of MCFCs and MCECs and developing strategies to mitigate potential challenges associated with high-temperature operations.

Thus, this work aims to investigate the effect of temperature on electrode reactions employing the RA method. This will help to elucidate the previous works on MCECs using steady-state polarisation, electrochemical impedance, and ISA methods.

2. Experimental

2-1. Materials and Methods

The experimental configuration replicated the setup exclusively reprorted in a prior study [2]. The components for the MCCs were provided by the Korea Institute of Science and Technology (KIST). A single-cell assembly with an active electrochemical area of about 100 cm^2 was used. The HE is porous Ni alloy and the OE is *in-situ* oxidized porous NiO. More detailed properties of this assembly were listed in Table 1 of reference [1]. This assembly involved sandwiching electrolyte sheets and a matrix between the HE and OE, which were then enclosed with current collectors to form a single cell. Cell frames with gas flow channels were used to secure the assembly, which was then compressed and heated using a compressor equipped with heating rods.

A gaseous mixture of H_2/CO_2 = 0.3/0.3 L min^{-1} pretreated in a humidifier at 349 K was supplied to HE, producing 0.4 L min^{-1} of H_2O. The OE received a mixture of air/CO_2 = 0.621/0.261 L min^{-1}. Gas flow rates were monitored by Mass Flow Controllers (MFCs) under standard conditions. The gases were distributed through a 4.8 mm inner diameter stainless steel pipe.

The HE received H_2 and CO_2 in the RA analysis, while the OE was supplied with O_2 and CO_2. The change in cell voltage due to the addition of reactant gases was measured under three current conditions: 0 mA cm^{-2} (Open-Circuit State, OCS), 150 mA cm^{-2} (fuel cell mode), and –150 mA cm^{-2} (electrolysis cell mode). Reactant gas inlet ports were positioned approximately 3.5 meters ahead of the cell [2]. One MFC regulated the additional reactant gas flow rate, ranging between 0.1 and 0.6 L min^{-1}. A LeCroy WaveSurfer 64Xs-A oscilloscope was used to simultaneously capture the voltage signals from the cell and the MFC rate.

2-2. Reactant Gas Addition (RA) Method Analysis

A detailed analysis of the RA method was explicitly discussed in previous work [2]; hence, this section will briefly discuss it. MCFCs and MCECs were primarily operated under a current-controlled state. Their cell output voltage (V) under a current was lower than open-circuit voltage (E_{OCV}) for fuel cells but higher than electrolysis cells due to overpotential (η_T). As shown below, the V, E_{OCV}, and η_T were related in Eq. (1) expression for MCFC and MCEC.

$$V = E_{OCV} \pm \eta_T \tag{1}$$

$$E_{OCV} = E^0 + \frac{RT}{2F}\ln\left(\frac{(p_{H_2})(p_{CO_2})_{OE}(p_{O_2})^{0.5}}{(p_{H_2})(p_{CO_2})_{HE}}\right) \tag{2}$$

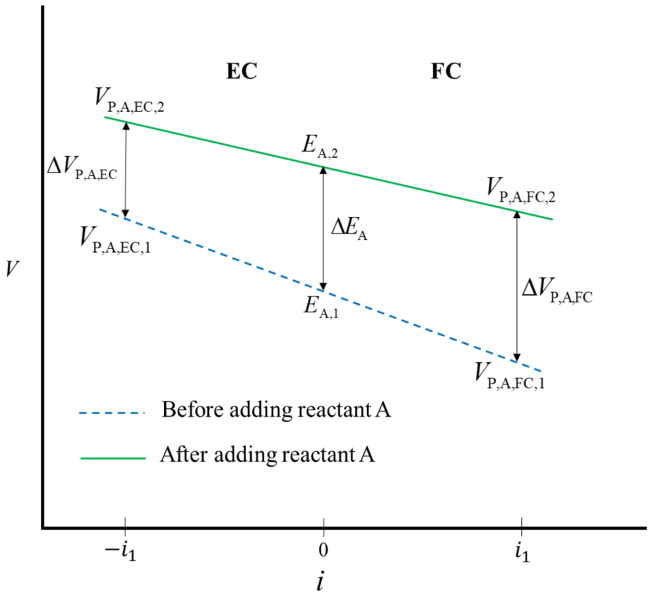

Fig. 1. Schematic illustration of the expected voltage trendlines (green and blue) and voltage changes caused by adding reactant *A* to an electrode in open-circuit (ΔE_A) and polarisation states ($\Delta V_{P,A}$).

$$\eta_T = \eta_{IR} + \eta_{HE} + \eta_{OE} \tag{3}$$

η_{IR} was the ohmic loss whereas η_{OE} and η_{HE} denoted the overpotential at the OE and HE, respectively.

In RA method, a reactant gas introduced to an electrode altered the voltage in open-circuit and polarisation states, as illustrated in Fig. 1. Adding reactant species A to an electrode at an OCS changed the E_{OCV} from $E_{A,1}$ to $E_{A,2}$ due to the partial pressure changes of reactant gases. In contrast, at the polarisation state (PS), the cell voltage (V) will change from $V_{P,A,1}$ to $V_{P,A,2}$. The effect of the added reactant A on the electrode's overpotential can be expressed for both fuel cell and electrolysis cell modes, as shown in Eqs. (4) and (5), respectively [2]. Positive and negative values of ΔV_A suggested varied impacts on mass transfer rate and overpotential due to the added reactant, while zero ΔV_A implied no effect.

$$\Delta V_{A,FC} = \Delta V_{P,A} - \Delta E_A = \eta_{A,1} - \eta_{A,2} \tag{4}$$

$$\Delta V_{A,EC} = \Delta E_A - \Delta V_{P,A} = \eta_{A,2} - \eta_{A,1} \tag{5}$$

where $\eta_{A,1}$ and $\eta_{A,2}$ were the cell overpotential before and after adding reactant A to an electrode, respectively.

3. Results and Discussion

3-1. Hydrogen Electrode

Fig. 2 illustrated the impact of adding 0.6 L min^{-1} of H_2 and CO_2 to cells operating in FC and EC modes at 823 K and 973 K temperatures. The cells exhibited remarkable and stable performances, with an E_{OCV} around 1 V and polarisation voltages of 0.6 V (FC mode) and 1.3 V (EC mode) at 823 K and 0.8 V (FC mode) and 1.1 V (EC mode) at 973 K as shown in Fig. 2. Time regions labelled 'A'

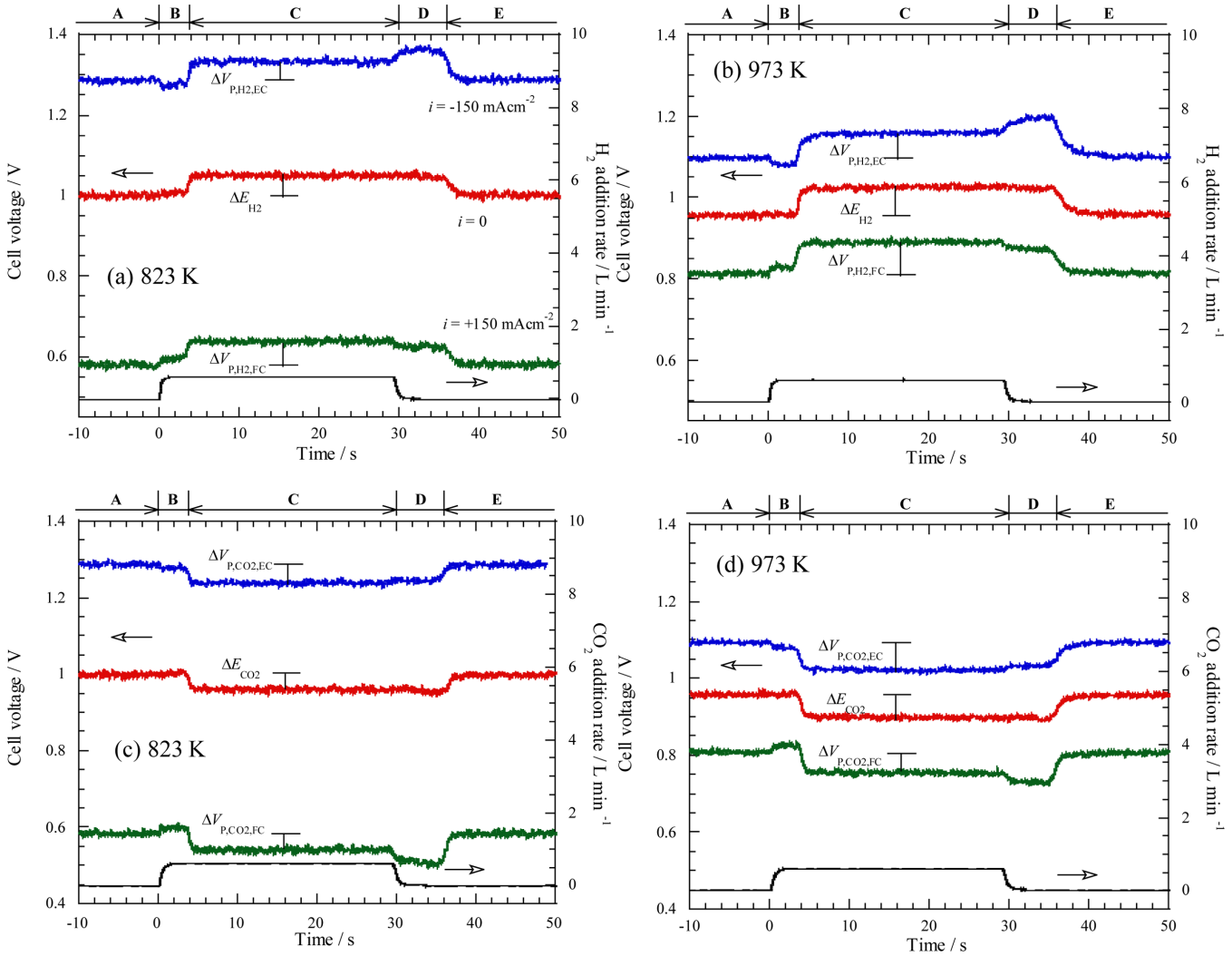

Fig. 2. Voltage behaviours at 823 K and 973 K with the addition of 0.6 L min^{-1} H_2 (a & b) and CO_2 (c & d) to the HE of MCCs operated in FC (i = 150 mA cm^{-2}) and EC (i = –150 mA cm^{-2}) modes. (1 atm, HE: H_2/CO_2 = 0.3/0.3 L min^{-1} + 40% H_2O, OE: air/CO_2 = 0.621/0.261 L min^{-1}).

to 'E' have been extensively discussed by this research group [2]. However, time region 'C', where changes in the reactant partial pressure and flow rate occured, was particularly interesting in this work. The effect of the added reactant species on the electrode overpotential can be determined using the relation of Eqs. (4) and (5) for cells operated in FC and EC modes, respectively. Fig. 2 revealed that the E_{OCV} value obtained at 973 K (0.96 V) was lower than at 823 K (1.0 V) due to the dependence of the E^0 on temperature. In addition, Figs. 2(a) and (b) indicated that adding H_2 gas to the HE increased the E_{OCV} in the 'C' region due to the increased H_2 partial pressure, as per Eq. (2), at all temperatures. Similar to the OCS, the polarisation voltage in the 'C' regions of Figs. 2(a) and (b) were seen to increase. However, the voltage increase at PS was more pronounced than at OCS in FC mode, while the reverse was seen in EC mode. Consequently, the effect of H_2 addition on electrode overpotential ΔV_{H_2} in Figs. 2(a) and (b) were positive at all temperatures according to Eqs. (4) and (5). The positive values of $\Delta V_{H_2,FC}$ and $\Delta V_{H_2,EC}$ signified a reduction in H_2-inducing mass transfer resistance.

In contrast to H_2 addition, the addition of CO_2 resulted in a voltage decrease in the 'C' region at both OCS and PS, as seen in Figs. 2(c) and (d). The reduction in E_{OCV} can be explained by Eq. (2) due to increased CO_2 partial pressure at the HE. Numerically, the voltage decrease in FC mode ($\Delta V_{P,CO_2,FC}$) was smaller than at OCS (ΔE_{CO_2}), resulting in a positive $\Delta V_{CO_2,FC}$ regardless of temperature. Conversely, the voltage decrease in EC mode ($\Delta V_{P,CO_2,EC}$) was numerically more significant than ΔE_{CO_2} at all temperatures, leading to positive values of $\Delta V_{CO_2,FC}$. This indicated that the CO_2 addition reduced the mass transfer resistance at the HE, enhancing the mass transfer rate in both FC and EC modes. This was in well agreement with the results of previous work, which demonstrated that CO_2 participated in the H_2 consumption (FC) and evolution (EC) reactions with molten carbonate electrolytes and CO_2 deficiency results in the mass transfer resistance and overpotential increase [2,3].

Fig. 3 displayed trend values for $\Delta V_{H_2,FC}$, $\Delta V_{H_2,EC}$, $\Delta V_{CO_2,FC}$, and $\Delta V_{CO_2,EC}$ at different temperatures. The impact of H_2 addition was more pronounced in FC mode than in EC mode, while the opposite

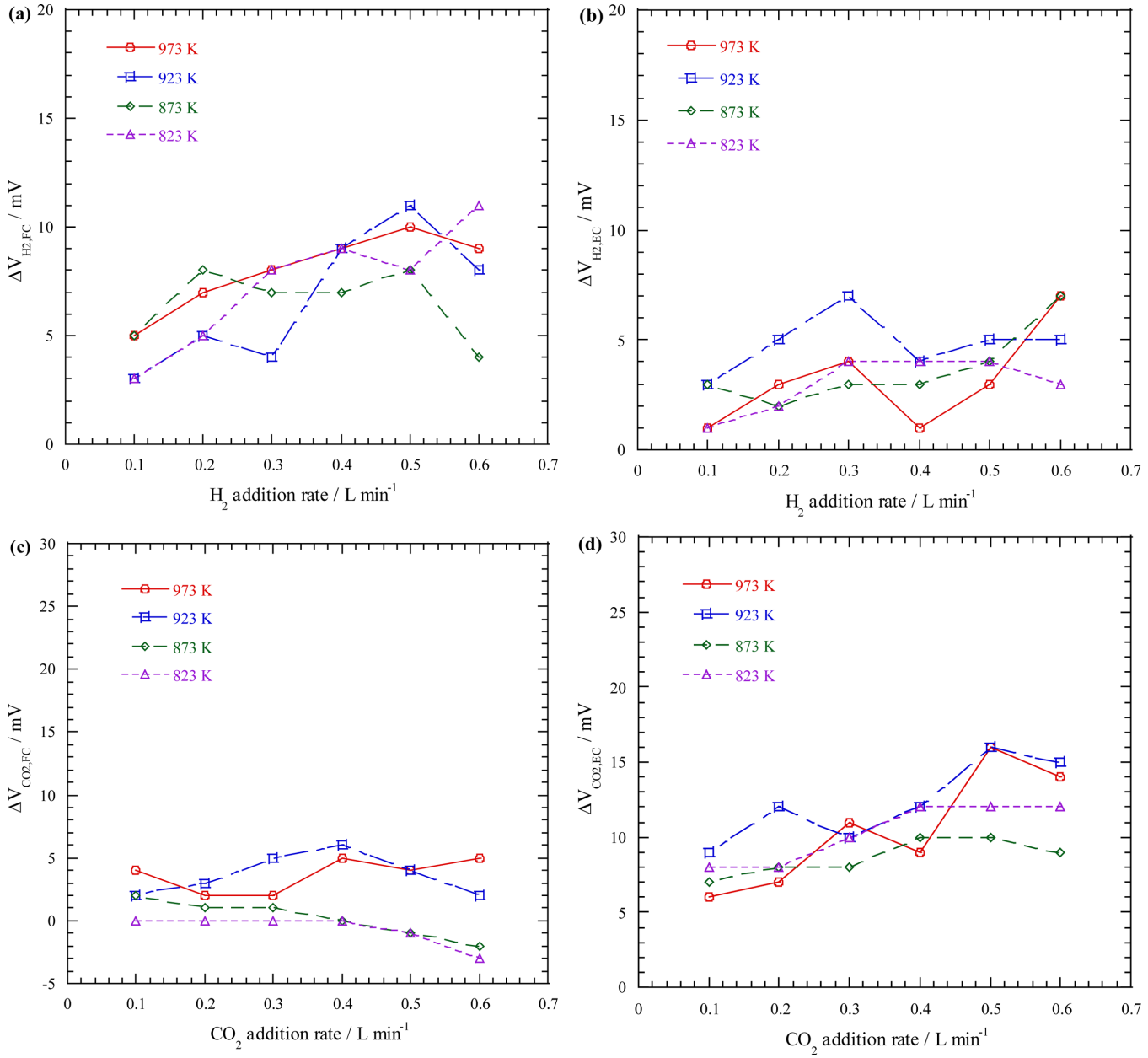

Fig. 3. (a) $\Delta V_{H_2,FC}$, (b) $\Delta V_{H_2,EC}$, (c) $\Delta V_{CO_2,FC}$, and (d) $\Delta V_{CO_2,EC}$ obtained at the HE from the difference between ΔE_A and $\Delta V_{P,A}$ in Fig. 2 at various temperatures for varied H_2 and CO_2 addition rates. (1 atm, HE: H_2/CO_2 = 0.3/0.3 L min^{-1} + 40% H_2O and OE: air/CO_2 = 0.621/0.261 L min^{-1}).

holds for CO_2 addition. Consequently, in EC mode, CO_2 was identified as a primary contributor to HE gas-phase mass transfer overpotential compared to H_2 at all temperatures, aligning with previous findings by this research group [2]. In MCEC, where CO_2 was consumed at HE to produce H_2 gas and carbonate ions (CO_3) (Eq. 6), $\Delta V_{CO_2,EC}$ was expected to be more significant than $\Delta V_{H_2,EC}$.

$$H_2 = CO_3^{2-} \underset{}{\overset{FC}{\rightleftharpoons}} CO_2 + H_2O + 2e^- \tag{6}$$

$$\eta_{mt,HE} = \sum_A \eta_A = \sum_A \frac{iR^2T^2\phi}{an^2F^2k_{G,A}p_{0,A}} \tag{7}$$

where a was the geometrical surface area, n was the number of electrons, p_0 was the gas bulk pressure, k was the mass transfer constant, ϕ was the Thiele modulus, and the subscripts G and mt denoted the gas-phase and mass transfer.

Comparison with previous research by Lee revealed a significant $\Delta V_{CO_2,FC}$ compared to $\Delta V_{H_2,FC}$ in the typical fuel gas composition (H_2:CO_2:H_2O = 0.69:0.17:0.14 atm) at all temperatures [7]. Lee attributed this behaviour to the low flow rate of CO_2 in the inlet fuel, *i.e.,* about 0.043 L min^{-1} CO_2 compared to the high H_2 flow rate of 0.172 L min^{-1}. In contrast, our study employed an equal flow rate for H_2 and CO_2 gases, *i.e.*, 0.3 L min^{-1} each, resulting in an insignificant $\Delta V_{CO_2,FC}$ comparable to $\Delta V_{H_2,FC}$. Notably, positive values of $\Delta V_{H_2,FC}$, $\Delta V_{H_2,EC}$, $\Delta V_{CO_2,FC}$, and $\Delta V_{CO_2,EC}$ indicated that the addition of H_2 and

CO_2 gases reduced the HE gas-phase mass transfer overpotential in both operation modes.

Despite the expectations based on electrochemical reactions, no clear temperature dependence was observed in Fig. 3 for $\Delta V_{H_2,FC}$, $\Delta V_{H_2,EC}$, $\Delta V_{CO_2,FC}$, and $\Delta V_{CO_2,EC}$. Increased temperature typically facilitates reactions in electrode pores, introducing a Pore Diffusion Resistance (PDR) phenomenon, which was represented using the Thiele modulus in the electrode overpotential in Eq. (7). However, the rise in temperature from 823 K to 973 K did not lead to significant changes in ΔV_A values as seen in Fig. 3, contrary to results by Lee [7] for MCFC in the same temperature range. The author reported a clear temperature dependence on $\Delta V_{H_2,FC}$ and $\Delta V_{CO_2,FC}$. The observed lack of temperature dependence in our study can be attributed to the substantial inlet feed flow rate (1 L min^{-1}) and very high CO_2 and H_2O compositions (H_2:CO_2:H_2O = 0.3:0.3:0.4 atm) to reduce the mass transfer resistance and overpotential. Lee's work involved lower flow rates (0.254 L min^{-1}) and lower CO_2 and H_2O compositions (H_2:CO_2:H_2O = 0.69:0.17:0.14 atm), resulting in higher mass transfer resistance and overpotential [7]. The maximum $\Delta V_{H_2,FC}$ and $\Delta V_{CO_2,FC}$ values were notably smaller than those reported by Lee, *ca.* 45 mV and 60 mV for ref. [7] and 11 mV and 6 mV in this work, respectively. Additionally, Lee's investigation of overpotential as a function of HE gas composition in MCFC verified less significant $\Delta V_{H_2,FC}$ and $\Delta V_{CO_2,FC}$ values for compositions with higher H_2 gas and CO_2 flow rates, respectively [15].

The uncertainty of overpotential dependence on temperature, as shown in Fig. 3, also contradicted the earlier results of the ISA method that showed higher temperature has a larger overpotential at the HE of EC mode [3]. The ISA method used total flow rate change by adding inert gas without varying partial pressures of reactants to measure overpotential. Moreover, the overpotential measured by the ISA method was the sum of the overpotential caused by each reactant gas. On the other hand, the RA method only reflected overpotential variation due to each reactant gas. In addition, the high CO_2 and H_2O composition reduced mass transfer resistance and overpotential due to the gas species in this work. Therefore, it can be suggested that the ambiguous temperature dependence observed for $\Delta V_{H_2,FC}$, $\Delta V_{H_2,EC}$, $\Delta V_{CO_2,FC}$, and $\Delta V_{CO_2,EC}$ in Fig. 3 can be attributed to significantly reduced HE gas-phase mass transfer resistance and overpotential caused by the substantial inlet feed flow rate and relatively high CO_2 and H_2O partial pressures.

3-2. Oxygen Electrode

Fig. 4 illustrated the voltage responses induced by introducing 0.6 L min^{-1} of CO_2 to OE at 823 K (a) and 973 K (b) and the same amount of O_2 at 823 K (c) and 973 K (d) to OE in the FC and EC modes. Like Fig. 2, the authors were particularly interested in the 'C' time region. In Fig. 4, it was observed that the additions of O_2 and CO_2 did not result in a significant increase in E_{OCV} at all temperatures compared to Fig. 2. Specifically, in the case of CO_2 addition at PS in FC mode, a negative voltage shift at 823 K (Fig. 4a) and a positive one at 923 K (Fig. 4b) was observed. Since the solubility of CO_2 in carbonate melts was higher than that of O_2, the CO_2 addition caused reduction in the O_2 species at the OE. This reduction, in turn, increased the O_2-inducing mass transfer resistance. The liquid-phase mass transfer resistance at the OE ($R_{L,OE}$) was controlled primarily by CO_2 and superoxide ion (O_2^-), with the O_2 ion being the dominant rate-limiting species due to lower O_2 solubility. Therefore, the negative voltage shift at 823 K in Fig. 4(a) could be attributed to the increased mass transfer resistance of O_2 due to reduced partial pressure and lower solubility in the carbonate melt. Conversely, the positive voltage shift at 973 K was linked to increased O_2 solubility, mitigating the O_2-inducing mass transfer resistance despite the amount of CO_2 added. Lee also observed similar negative and positive voltage shifts at the same experimental conditions [8] in 100 cm^2 class MCFCs.

In EC mode, CO_2 addition significantly increased the voltage at all temperatures, as shown in Figs. 4(a) and (b). At the OE, the carbonate ions decomposed into CO_2 and O_2 gases during the EC mode of operation (Eq. 8). However, it has been indicated in previous work that the liquid-phase mass transfer resistance of the OE in EC mode depends on partial pressures of both O_2 and CO_2 gas [3]. Thus, adding CO_2 reduced the partial pressure of O_2, resulting in fewer O_2^- ions in the melt. Since O_2 ions controlled the $R_{L,OE}$, CO_2 addition will increase $R_{L,OE}$ and the overall overpotential, as seen in Figs. 4(a) and (b) at the temperatures of 823 and 973K.

$$\frac{1}{2}O_2 + CO_2 + 2e^- \underset{EC}{\overset{FC}{\rightleftharpoons}} CO_3^{2-} \tag{8}$$

When O_2 was added in FC mode, voltage increased at 823 K (Fig. 4c) and 973 K (Fig. 4d), with substantial increase at 823 K. This significant increase observed in the time region 'C' at 823 K suggested a substantial O_2-inducing mass transfer resistance, primarily owing to a rise in $R_{L,OE}$ at lower temperatures. The gas-phase mass transfer resistance at the OE was less temperature-dependent, while the $R_{L,OE}$ depends strongly on temperature, especially in FC mode, as indicated by the ISA method [3]. Thus, the behaviour observed in Fig. 4(c) at 823 K can be attributed to the increased $R_{L,OE}$. On the other hand, a rise in temperature caused the solubility of the O_2 species to increase in the carbonate electrolyte, thereby reducing the $R_{L,OE}$ which was seen in Fig. 4(d) as a reduced voltage shift at 973 K compared to 823 K.

In summary, Fig. 4 suggested that adding O_2 reduced mass transfer resistance (positive ΔV_{O_2}) at all temperature modes, while CO_2 addition increased mass transfer resistance (negative ΔV_{O_2}) in both FC and EC modes.

Fig. 5 showed trend values for $\Delta V_{O_2,FC}$, $\Delta V_{O_2,EC}$, $\Delta V_{CO_2,FC}$, and $\Delta V_{CO_2,EC}$ at temperatures of 823 K, 873 K, 923 K, and 973 K. Examining Fig. 5(a), a significant temperature dependence of $\Delta V_{O_2,FC}$ was evident, aligning with the findings of Lee [8]. While Lee [8] reported a maximum $\Delta V_{O_2,FC}$ value of approximately 170 mV at 823 K, our work achieved about 108 mV, indicating robust cell performance. The high $\Delta V_{O_2,FC}$ values observed in Fig. 5(a) imply increased O_2-inducing mass transfer resistance due to the low solubility of O_2

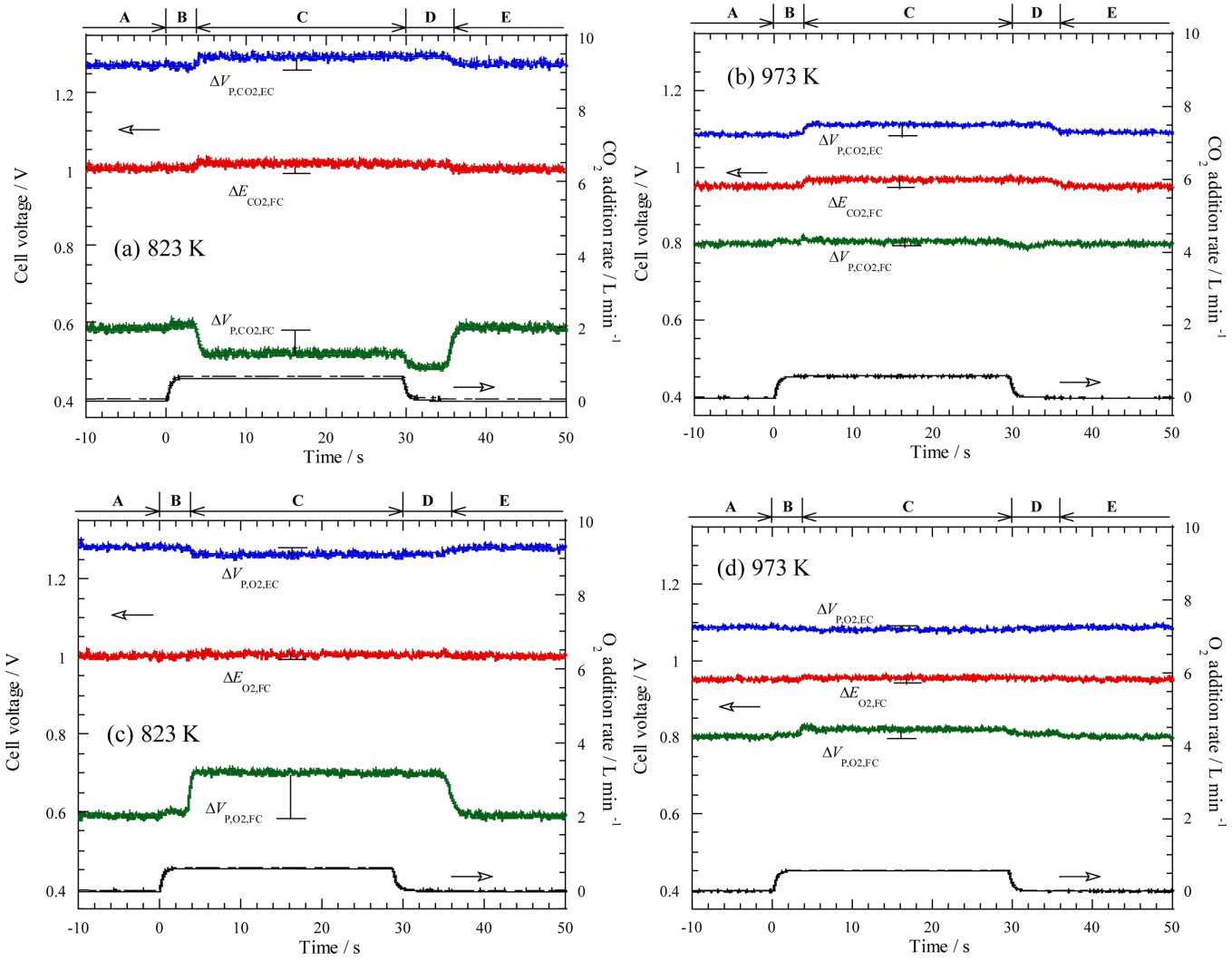

Fig. 4. Voltage behaviours at 823 K and 973 K with the addition of 0.6 L min^{-1} CO_2 (a & b) and O_2 (c & d) to the OE of MCCs operated in FC and EC modes. (1 atm, HE: H_2/CO_2 = 0.3/0.3 L min^{-1} + 40% H_2O, OE: air/CO_2 = 0.621/0.261 L min^{-1} and i = ±150 mA cm^{-2}).

species in the carbonate electrolyte. As temperature enhanced from 823 K to 973 K, $\Delta V_{O_2,FC}$ declined significantly to an average of 13 mV, indicating a reduced O_2-inducing mass transfer resistance attributed to increased O_2 solubility.

Contrary to Fig. 5(a), Fig. 5(b) displayed a clear but not distinct temperature dependence of $\Delta V_{O_2,EC}$. Both $\Delta V_{O_2,FC}$ and $\Delta V_{O_2,EC}$ were positive, indicating that addition of O_2 reduced O_2-inducing mass transfer resistance and, consequently, the electrode overpotential. Additionally, the $\Delta V_{O_2,EC}$ values were much smaller than $\Delta V_{O_2,FC}$, especially at 823 K and 873 K, reflecting the already reduced O_2-inducing mass transfer resistance caused by the O_2 produced by the decomposition of CO_3^{2-} ions in EC mode. In FC mode, where O_2 was consumed, larger $\Delta V_{O_2,FC}$ values were observed, aligning with observations in Fig. 5(a). The trends in Figs. 5(a) and (b) were similar to previous reports by our research group for MCCs operated at 923 K [2].

Adding CO_2 to the OE results in negative values for $\Delta V_{CO_2,FC}$ and $\Delta V_{CO_2,EC}$ as in Figs. 5(c) and (d), indicating increased overpotential due to elevated mass transfer resistance in both modes. As explained earlier in Figs. 4 (a) and (b), adding CO_2 to the OE increased the O_2-inducing mass transfer resistance by decreasing the partial pressure of O_2 species. Similar to Fig. 5(a), $\Delta V_{CO_2,FC}$ decreased with increasing temperature, with 973 K exhibiting the smallest $\Delta V_{CO_2,FC}$ values due to the enhanced O_2 solubility in the carbonate melt at high temperatures, as noted in Fig. 5(c). A precise temperature dependence of $\Delta V_{CO_2,FC}$ was observed in Fig. 5(c), while no clear temperature dependence was observed for $\Delta V_{CO_2,EC}$ in Fig. 5(d). Previous reports from our group indicated the liquid-phase mass transfer resistance of OE in EC mode to be relatively small compared to FC and independent of temperature [3] due to insignificant changes in the partial pressures of CO_2 and O_2 by the generation of those gases in EC mode. In addition, a negligible gas-phase mass transfer resistance due to flow rate changes was reported for the OE in EC mode *via* the ISA method [1]. Thus, the relatively small O_2-inducing liquid-phase mass transfer resistance contributed to smaller numerical values for $\Delta V_{CO_2,EC}$ compared to $\Delta V_{CO_2,FC}$, at all temperatures.

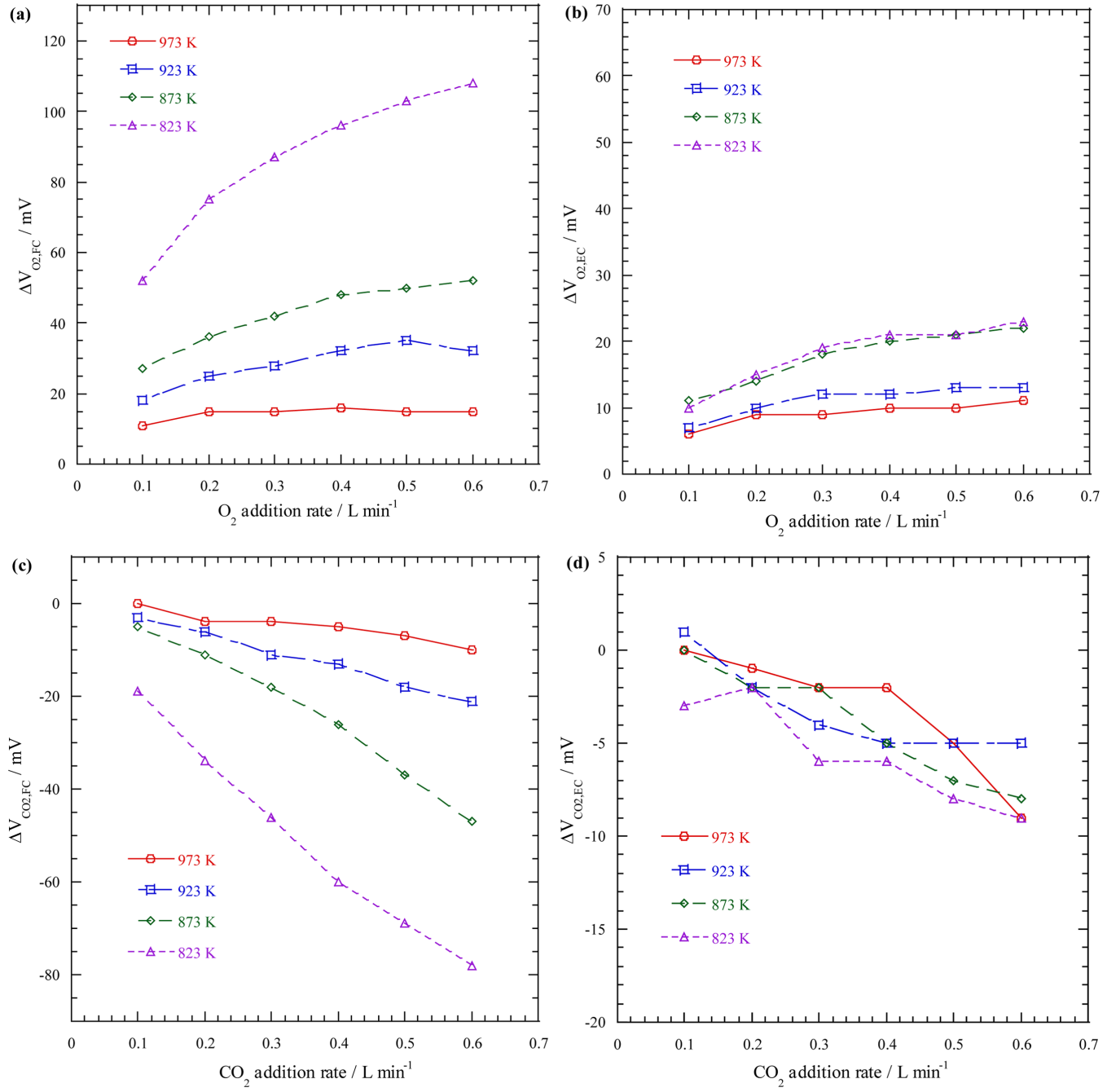

Fig. 5. (a) $\Delta V_{O_2,FC}$, (b) $\Delta V_{O_2,EC}$, (c) $\Delta V_{CO_2,FC}$, and (d) $\Delta V_{O_2,EC}$ obtained at the OE from the difference between ΔE_A and $\Delta V_{P,A}$ in Fig. 4 at various temperatures for varied O_2 and CO_2 addition amounts. (1 atm, HE: H_2/CO_2 = 0.3/0.3 L min^{-1} + 40% H_2O and OE: air/CO_2 = 0.621/0.261 L min^{-1}).

4. Conclusion

This research delved into the influence of temperature on electrode reactions within MCCs using the RA method. Building on comparisons from previous studies, this investigation explored the multifaceted aspects of temperature dependence, including thermodynamics, reaction kinetics, and mass transfer in 100 cm^2 class MCCs operating reversibly in EC and FC modes. The focus extended to the HE and OE, emphasising the step addition of H_2, CO_2, and O_2 gases.

Remarkably, the study revealed that the H_2 and CO_2 additions at the HE reduced the overpotential when operated in EC and FC modes, with H_2 and CO_2 being the primary causative species for HE overpotential in the FC and EC modes, respectively. Additionally, no clear temperature dependence was observed for H_2 and CO_2 addition effects in both modes, owing to the high flow rates of supplied reactants.

The findings regarding the OE demonstrated precise temperature dependence on O_2 and CO_2 additions in FC mode, while unclear temperature dependence was observed in EC mode, especially for CO_2 addition. Furthermore, O_2 and CO_2 exhibited contrasting effects

in both modes, with O_2 addition leading to reduced OE overpotential due to an increased concentration of superoxide ions in the melts. On the other hand, CO_2 addition enhanced OE overpotential by decreasing the partial pressure of O_2 species.

Moreover, the study underscored the significant role of reactant gas addition in shaping electrode reactions, laying the groundwork for further advancements in utilising MCCs for efficient power generation and the conversion of surplus electricity into chemical fuels.

Acknowledgements

This research was supported by the New & Renewable Energy Core Technology Programme of the Korea Institute of Energy Technology Evaluation and Planning (KETEP), granted financial resources from the Ministry of Trade, Industry, and Energy, Republic of Korea (No. 20213030040080).

Nomenclature

Symbol

A : Reactant species [CO_2, H_2, O_2, and H_2O]
a : Geometrical surface area of the electrode [cm^2]
E_{OCV} : Open-circuit voltage [V]
E^0 : Standard potential [V]
F : Faraday constant [C mol^{-1}]
i : Current [A]
k : Mass transfer constant [cm s^{-1}]
n : Number of electrons involved in the electrochemical reactions
p : Partial pressure [atm]
p_0 : Bulk gas pressure [atm]
R : Molar gas constant [J K^{-1} mol^{-1}]
T : Absolute temperature [K]
V : Cell output voltage [V]
ΔE_A : Voltage gap between regions 'A' and 'C' in an open-circuit state [V]
$\Delta V_{P,A}$: Voltage gap between regions 'A' and 'C' in a polarisation state [V]
ΔV_A : Voltage difference between W_O and W_P due to adding an inert gas [V]

Greek letters

η : Overpotential [V]
ϕ : Thiele modulus

Subscripts

A : Reactant species
FC : Fuel cell
EC : Electrolysis cell
G : Gas-phase
HE : Hydrogen electrode
IR : Internal resistance
L : Liquid-phase
mt : Mass transfer
OCS : Open circuit state
OE : Oxygen electrode
PDR : Pore diffusion resistance
PS : Polarisation state
T : Total
1 : State before the addition of a reactant gas
2 : State after the addition of a reactant gas

References

1. Koomson, S. and Lee, C. G., "Comparison of Gas Phase Transport Effects Between Fuel Cell and Electrolysis Cell Modes of a 100 cm^2 Class Molten Carbonate Cell," *J. Electroanal. Chem.*, **925**, 116896(2022).
2. Koomson, S. and Lee, C.-G., "Reaction Characteristics of Molten Carbonate Cell Operated in Fuel Cell and Electrolysis modes with Reactant Gas Addition Method," *J. Electroanal. Chem.*, 117577 (2023).
3. Koomson, S., Bae, S. H., Kim, K. M. and Lee, C.-G., "Effect of Temperature on the Electrode Overpotential of Molten Carbonate Electrolysis and Fuel Cells with Inert-gas Step Addition Method," *J. Electroanal. Chem*., **950**, 17844(2023).
4. Saito, T., Itoh, Y., Nishioka, M. and Miyake, Y., "Effect of Operating Temperature on the Performance of Molten-carbonate Fuel Cells," *J. Power Sources*., **36**, 69-77(1991).
5. Morita, H., Komoda, M., Mugikura, Y., Izaki, Y., Watanabe, T., Masuda, Y. and Matsuyama, T., "Performance Analysis of Molten Carbonate Fuel Cell Using a Li/Na Electrolyte," *J. Power Sources*., **112**, 509-518(2002).
6. Musa, A., Steeman, H.-J. and De Paepe, M., The Effect of Operating Temperature on the Performance of Molten Carbonate Fuel Cell systems, in: 16th World Hydrog. Energy Conf., International Association for Hydrogen Energy, 2006.
7. Lee, C. G., "Influence of Temperature on the Anode Reaction in a Molten Carbonate Fuel Cell," *J. Electroanal. Chem*., **785**, 152-158(2017).
8. Lee, C. G., "Effect of Temperature on the Cathodic Overpotential in a Molten Carbonate Fuel Cell," *J. Electroanal. Chem*., **701**, 36-42(2013).
9. Hu, L., Rexed, I., Lindbergh, G., and Lagergren, C., "Electrochemical Performance of Reversible Molten Carbonate Fuel Cells," *Int. J. Hydrogen Energy*., **39**, 12323-12329(2014).
10. Hu, L., Lindbergh, G., Lagergren, C., "Operating the Nickel Electrode with Hydrogen-lean Gases in the Molten Carbonate Electrolysis Cell (MCEC)," *Int. J. Hydrogen Energy*., **41**, 18692-18698(2016).
11. Hu, L., Lindbergh, G. and Lagergren, C., "Electrode Kinetics of the Ni Porous Electrode for Hydrogen Production in a Molten Carbonate Electrolysis Cell (MCEC)," *J. Electrochem. Soc*., **162**, F1020-F1028(2015).
12. Hu, L., Lindbergh, G. and Lagergren, C., "Electrode Kinetics of the NiO Porous Electrode for Oxygen Production in the Molten Carbonate Electrolysis Cell (MCEC)," *Faraday Discuss*., **182**,

493-509(2015).
13. Perez-Trujillo, J. P., Elizalde-Blancas, F., Della Pietra, M. and McPhail, S. J., "A Numerical and Experimental Comparison of a Single Reversible Molten Carbonate Cell Operating in Fuel Cell Mode and Electrolysis Mode," *Appl. Energy.*, **226**, 1037-1055 (2018).
14. Audasso, E., Kim, K. I., Accardo, G., Kim, H. S. and Yoon, S. P., "Investigation of Molten Carbonate Electrolysis Cells Performance for H_2 Production and CO_2 Capture," *J. Power Sources*., **523**, 231039(2022).
15. Lee, C. G., Hwang, J. Y., Oh, M., Kim, D. H., Lim, H. C., "Overpotential Analysis with Various Anode Gas Compositions in a Molten Carbonate Fuel Cell," *J. Power Sources*., **179**, 467-473(2008).

Authors

Samuel Koomson: Post Doc, Department of Chemical & Biological Engineering, Hanbat National University, Daejeon 34158, Korea; samuelkoomson18@yahoo.com

Choong-Gon Lee: Professor, Department of Chemical & Biological Engineering, Hanbat National University, Daejeon 34158, Korea; leecg @hanbat.ac.kr